Industrial Crops & Products 200 (2023) 116838

Contents lists available at ScienceDirect

Industrial Crops & Products

journal homepage: www.elsevier.com/locate/indcrop

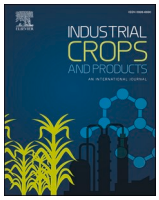

Economic analysis of the supercritical fluid extraction of lupane-triterpenoids from *Acacia dealbata* Link bark

Vítor H. Rodrigues, Inês Portugal *, Carlos M. Silva *

CICECO – Aveiro Institute of Materials, Department of Chemistry, University of Aveiro, 3810-193 Aveiro, Portugal

ARTICLE INFO

Keywords:
Acacia dealbata
Bark
Economic analysis
Lupenyl acetate
Supercritical fluid extraction
Triterpenoids

ABSTRACT

The supercritical fluid extraction of *Acacia dealbata* Link. bark was performed with carbon dioxide at different pressures (10–30 MPa), temperatures (40–80 °C), and cosolvents contents (0–10 wt% of ethyl acetate or ethanol) to analyse their effect on various performance indicators whose best values were: total extraction yield of 1.57 wt %; lupenyl acetate (LA) and lupenone (Lu) extraction yields of 777.5 mg kg_{bark}^{-1} and 679.8 mg kg_{bark}^{-1}; and LA and Lu extract concentrations of 15.8 wt% and 12.8 wt%. Two extraction curves were measured, and an economic analysis was accomplished. The impact of pressure, temperature, cosolvent content, and extraction time on the cost of manufacturing (COM) and productivity were evaluated, reaching a minimum of 52.3 € $kg_{extract}^{-1}$. A sensitivity analysis showed that the electricity price is the most impactful variable on the COM. Overall, the increase of pressure, temperature and cosolvents content favoured the productivity, decreasing the production cost.

1. Introduction

Today's society is ever more concerned with environmental issues, such as the sustainability of products and processes. This mindset motivates an efficient management of natural resources and the transition from a fossil fuel-based economy to a bioeconomy, where chemicals, fuels, energy and overall products are obtained from renewable sources (like vegetable biomass), as preconized by the biorefinery concept (Fereira, 2017).

Forest-based industries are one of the main sources for residual biomass, generated during logging and forests maintenance, but also during wood pretreatment and cleaning. This is the case for *E. globulus* Labill. and *A. dealbata* Link. trees, where the former is the main source of wood for pulp and paper industries in southwestern Europe (Portugal and Spain) and the latter is an invasive species that can be found in eucalypt plantations (Cerasoli et al., 2016; Correia et al., 2020). Even though the pulp and paper mills comprise energy and chemicals recovery cycles from residual streams, such as the production of chemicals from liquors, it has been demonstrated that the production of energy from residual biomass does not recover a fraction of potential added-value compounds found in the bark, leaves, flowers and wood of either *E. globulus* Labill. (de Melo et al., 2012; de Melo et al., 2014; Domingues et al., 2012b; Rodrigues et al., 2021c, 2018; Santos et al., 2012) or *A. dealbata* Link. (López-Hortas et al., 2021; Oliveira et al., 2020; Sarkar et al., 2017). These compounds can be recovered by green extraction technologies, like supercritical fluid extraction (SFE), without compromising the mill's energy production stage.

The use of SFE technology potentiates the value of the extracts, especially when using supercritical carbon dioxide (SC-CO_2) as solvent, enabling the production of products distinct from those obtained by conventional extraction with organic solvents while retaining the natural character of the product (de Melo et al., 2017; Perrut, 2000). Moreover, since SFE technology is Generally Recognized as Safe (GRAS) the ensuing products can target the food, pharmaceutical and nutraceutical sectors, which has motivated its application to hundreds of vegetable matrices during the last decades (de Melo et al., 2014c). While the SFE research from *E. globulus* Labill. biomass has been thorough, from preliminary SFE assays and extracts characterization (de Melo et al., 2012; Domingues et al., 2012b), experimental optimization (Domingues et al., 2013; Santos et al., 2012), measurement and modeling of extraction curves (Domingues et al., 2012a), scale-up (de Melo et al., 2014b), and techno-economic analysis (V.H. Rodrigues et al., 2019), only recently did SFE research start for *A. dealbata* Link. (Casas et al., 2021; Rodrigues et al., 2021a, 2021b). Two main lupane-triterpenoids have been identified in *A. dealbata* Link. bark extracts, namely lupenyl acetate (LA) and lupenone (Lu), which derive

* Corresponding authors.
E-mail addresses: inesport@ua.pt (I. Portugal), carlos.manuel@ua.pt (C.M. Silva).

https://doi.org/10.1016/j.indcrop.2023.116838
Received 10 January 2023; Received in revised form 12 April 2023; Accepted 2 May 2023
Available online 16 May 2023

from lupeol and have therapeutic potential towards inflammation, virus infection, diabetes, cancer, and Chagas disease (Lucetti et al., 2010; Saleem, 2009; Xu et al., 2018). Following a previous SFE work with preliminary assays (Rodrigues et al., 2021a), it is still necessary to optimize the main operating conditions and measure SFE curves, to analyze the kinetics of the process and establish the scale-up criterion.

In this work, the bark of *A. dealbata* Link. was extracted by means of CO_2 under supercritical conditions using a high number of combinations of operating conditions, such as pressure, temperature and cosolvent (ethanol or ethyl acetate) content. The results were analyzed in terms of total extraction yield, LA and Lu yields and concentrations in the extracts, and the results were compared with Soxhlet extraction using dichloromethane. Using a scale-up criterion frequently applicable to the supercritical fluid extraction (SFE) of biomass where internal limitations to mass transfer are relevant – *e.g.*, *E. globulus* Link. bark (de Melo et al., 2014b), *Moringa oleifera* seeds (Martins et al., 2016), spent coffee grounds (de Melo et al., 2014a) – the impact of several operating conditions upon an industrial plant were economically evaluated to obtain a preliminary cost of the acacia bark SFE process. Accordingly, this essay contributes to the establishment of a forest-based biorefinery integrated in a pulp and paper mill to produce *green* bioactive extracts enriched in lupenyl acetate and lupenone.

2. Materials and methods

2.1. Chemicals

Carbon dioxide (CO_2, purity 99 %) was supplied by Air Liquid (Algés, Portugal). Ethanol (purity 99.5 %) and dichloromethane (purity 99.98 %) were supplied by Fisher Scientific (Leicestershire, United Kingdom). Ethyl acetate (purity 99 %) was supplied by VWR International (Fontenay-sous-Bois, France). Pyridine (purity 99.5 %), tetracosane (purity 99 %) N,O-Bis(trimethylsilyl)trifluoroacetamide (BSTFA, purity 98 %) and chlorotrimethylsilane (TMSCl, purity 99 %) were supplied by Sigma Aldrich (Madrid, Spain). Betulinic, oleanolic and ursolic acids (purity 98 %) were supplied by AK Scientific (Union City, USA), and lupenone (95 %) was supplied by Apollo Scientific Ltd (Stockport, United Kingdom).

2.2. Acacia dealbata Link. bark

The *A. dealbata* Link. bark used in this work was supplied by RAIZ—Forest and Paper Research Institute (Eixo, Portugal). It was collected in Porto/Valongo (Portugal) region during June 2020, from 10 years old *Acacia dealbata* Link. trees. The biomass consisted of long sections of bark that were cut in chips (size *ca.* 2 cm × 1 cm) and dried at 35 °C for 72 h, reducing the moisture content, expressed as mass fraction of water, $w_{H2O} = 9.6$ wt%. The dried bark chips were stored in closed bags and kept in the dark.

2.3. Soxhlet extraction

Soxhlet extractions of *A. dealbata* Link. bark were performed with dichloromethane due to its selectivity towards triterpenoids (Oliveira et al., 2020; Rodrigues et al., 2021a). The extractions were performed for 6 h using *ca.* 7 g of bark and 180 mL of solvent (see Table 1). Afterwards, the extracts were evaporated to dryness in a rotary evaporator, weighed for total extraction yield (η_{Total}) determination, and analysed by gas chromatography coupled to mass spectrometry (GC-MS) to evaluate triterpenoids yields (η_i) and extract concentrations (C_i). The extractions were performed in triplicate and the results presented correspond to the mean.

The experimental total percent yield, η_{Total} (wt.%), was calculated by Eq. (1), the individual extraction yields $\left(\eta_i, \text{mg kg}_{\text{bark}}^{-1}\right)$ of lupenyl acetate (LA) and lupenone (Lu) were calculated by Eq. (2), and the individual extract concentrations (C_i, wt%) of the two compounds were calculated by Eq. (3):

Table 1
List of Soxhlet extraction (with dichloromethane) and SFE experiments (with CO_2, pure or modified with ethyl acetate (EA) or ethanol (EtOH)), and the respective SFE cosolvent content, pressure, temperature, and supercritical fluid density. The mass of bark in the SFE experiments was 50.0 g and for Soxhlet was 7.0 g.

Run	Solvent	Cosolvent content (wt %)	Q_{CO_2} (g min^{-1})	P (MPa)	T (°C)	ρ_{SCF} (kg m^{-3})
SFE1	CO_2	0	12	20	40	826.20
SFE2	CO_2	0	12	20	80	586.13
SFE3	CO_2	0	12	30	60	817.04
SFE4_EA	CO_2 + EA	5	12	10	40	746.34
SFE5_EA	CO_2 + EA	5	12	10	80	265.29
SFE6_EA	CO_2 + EA	5	12	20	60	757.99
SFE7_EA	CO_2 + EA	5	12	30	40	915.99
SFE8_EA	CO_2 + EA	5	12	30	80	764.74
SFE9_EA	CO_2 + EA	10	12	10	60	630.02
SFE10_EA	CO_2 + EA	10	12	20	40	880.90
SFE11_EA	CO_2 + EA	10	12	20	80	694.90
SFE12_EA	CO_2 + EA	10	12	30	60	862.99
SFE4_EtOH	CO_2 + EtOH	5	12	10	40	743.46
SFE5_EtOH	CO_2 + EtOH	5	12	10	80	254.00
SFE6_EtOH	CO_2 + EtOH	5	12	20	60	750.69
SFE7_EtOH	CO_2 + EtOH	5	12	30	40	908.98
SFE8_EtOH	CO_2 + EtOH	5	12	30	80	755.18
SFE9_EtOH	CO_2 + EtOH	10	12	10	60	640.34
SFE10_EtOH	CO_2 + EtOH	10	12	20	40	872.20
SFE11_EtOH	CO_2 + EtOH	10	12	20	80	686.20
SFE12_EtOH	CO_2 + EtOH	10	12	30	60	852.22
SFE1_C1	CO_2	0	12	20	40	826.20
SFE1_C2	CO_2	0	18	20	40	826.20
Soxhlet	DCM	–	–	–	39.8 (*)	–

SFE6_EA and SFE6_EtOH were run in triplicate.
(*) – Dichloromethane (DCM) normal boiling temperature – NIST database.

$$\eta_{Total} = \frac{m_{extract}}{m_{dry\ biomass}} \times 100 \quad (1)$$

$$\eta_i = \frac{m_i}{m_{dry\ biomass}} \quad (2)$$

$$C_i = \frac{m_i}{m_{extract}} \times 100 \quad (3)$$

where $m_{dry\ biomass}$ is the mass of dry bark, $m_{extract}$ is the mass of extract weighed after solvent evaporation, and m_i is the mass of the triterpenoid being quantified.

2.4. Supercritical fluid extraction

Supercritical fluid extractions (SFE) were performed in a cylindrical 0.5 L lab scale extractor (12 cm of height, 7.3 cm of internal diameter), model Spe-ed™ from Applied Separations Inc. (USA). Cooled CO_2 was pressurized using a liquid pump (diaphragm pump) and heated to the extraction temperature in the pre-heating vessel. After reaching the desired pressure and temperature conditions, the extraction was started by opening the back-pressure regulator (BPR) valve. The supercritical fluid (SCF) was fed to the bottom of the extraction bed and flowed

upwards through the biomass (*A. delalbata* bark) bed. The outlet stream was depressurized in a cooled extract collector and bubbled in ethanol to ensure the precipitation of the extract from the gaseous CO_2. Ethanol was removed from the extracts by evaporation in a rotary evaporator until dryness. For the assays using cosolvent, an HPLC pump was used to mix it with the CO_2 before the extractor inlet and, at the end of the extraction, the cosolvent was removed along with the ethanol used for the extract collection.

A total of 25 extractions were performed, testing different conditions of pressure (10 MPa, 20 MPa, 30 MPa), temperature (40 °C, 60 °C, 80 °C) and cosolvent content expressed as mass fraction (0 %, 5 %, 10 %) using ethyl acetate or ethanol. Ethyl acetate was selected for this work in light of the improved concentrations of the triterpenoids LA and Lu obtained in a previous work (Rodrigues et al., 2021a), as well as the observed enhancement of η_{Total}, triterpenes yield, and extraction kinetics in the case of the SFE of vine leaves (de Melo et al., 2020). Ethanol was also tested as it is the reference cosolvent employed in SFE of vegetable matrices (M.M.R. de Melo et al., 2014c). For each experiment, the extractor was loaded with 50.0 g of bark and was percolated with a CO_2 flow rate of 12 g min^{-1} for 6 h. To evaluate the variability of the experimental results, two replicas were performed at the medium value of each condition (20 MPa, 60 °C, 5 wt% cosolvent) for the two cosolvents. Additionally, two extraction curves were performed at 20 MPa, 40 °C, and different flow rates, namely, 12 g min^{-1} (solvent to feed mass ratio of 86.4 kg kg^{-1}) and 18 g min^{-1} (solvent to feed mass ratio of 129.6 kg kg^{-1}), to assess the effect of flow rate and the extraction kinetics. The experimental conditions are summarized in Table 1 along with the supercritical fluid respective densities (ρ_{SCF}) obtained using the PC-SAFT (Gross and Sadowski, 2002; Zaird, 2022) equation of state for pure SC-CO_2 and SC-CO_2 plus ethanol, while the densities of SC-CO_2 modified with ethyl acetate were extrapolated from experimental data (Falco and Kiran, 2012).

2.5. Gas chromatography coupled to mass spectrometry

The extracts were analysed by GC–MS after trimethylsilylation according to a procedure described in the literature (de Melo et al., 2012; Domingues et al., 2012b). Briefly, for each extract an aliquot of 20 mg was analysed in duplicate (average results are reported) using a Trace Gas Chromatograph Ultra equipped with a DB-1 J&W capillary column (30 m × 0.32 mm i.d., 0.25 μm film thickness) and coupled with a Thermo DSQ mass spectrometer. Helium was the carrier gas (1.5 $mLmin^{-1}$) and the chromatographic conditions were as follows: furnace initial temperature of 80 °C for 5 min, heating ramp at 4 °Cmin^{-1} until 260 °C, heating ramp at 2 °Cmin^{-1} up to the final temperature of 285 °C, and then 10 min at this temperature; injector temperature of 250 °C; transfer-line temperature of 290 °C; split ratio equal to 1:50. The MS was operated in the electron impact mode with electron impact energy of 70 eV and data collected at a rate of 1 scans s^{-1}over a range of *m/z* from 33 to 750. The ion source was maintained at 250 °C. For quantification of LA and Lu in the extracts, tetracosane was used as internal standard while pure triterpenic acids (betulinic, oleanolic and ursolic acids) and lupenone were used as external standards.

2.6. Process design and simulation

Estimating the cost of manufacturing of a SFE unit requires information about the equipment, utilities, raw materials, and labor costs. The scale-up criterion adopted in this work was the constancy of the ratio between solvent flow rate and biomass weight, *i.e.* $Q_{CO_2} \quad w_{bark}^{-1} = \text{const}$, which is common for several biomasses and has been established in detail for the SFE of *E. globulus* bark (M.M.R. de Melo et al., 2014b) where the type of biomass and target compounds are identical (V.H. Rodrigues et al., 2019).

The scale selected for the simulations corresponds to an SFE unit of three parallel extractors of 1 m^3 each, so that it can process an *A. dealbata* bark amount equivalent of 5–10 % of the *E. globulus* bark generated in a medium-size pulp and paper mill, located in Aveiro, Portugal. Two layouts were designed, one for the operation with pure SC-CO_2 (see Fig. 1 Process A) and a second one for SC-CO_2 modified with ethanol or ethyl acetate (see Fig. 1 Process B), based on previous works (de Melo et al., 2014a; V.H. Rodrigues et al., 2019). The operating conditions change several times during the CO_2 path along the cycle. In the case of Process A, there are two pressure regions: (i) the low pressure region, which encompasses the units after the BPR valve and before the CO_2 pump, namely, the separator, condenser and storage tank; (ii) the high pressure region, which comprises the pump, heater and extractor. Additionally, a compressor was also considered for the recovery of the CO_2 that exists in the system before unloading (*i.e.*, opening the extractor) from the operating pressure down to 0.5 MPa. The introduction of a cosolvent (Process B) requires an additional evaporator and separator for the extract recovery and solvent separation, as well as a dedicated cosolvent liquid pump and storage tank. In this case, the evaporator, second separator and storage tank belong to a third region, at 0.1 MPa, which encompasses the equipment starting after the valve in the bottom stream of the first separator (ATMVALVE) and before the cosolvent pump (COSPUMP).

The simulation of these layouts was carried out in ASPEN plus software using *RK-Aspen* method to retrieve the information necessary on utilities consumption. In order to assist vapor-liquid equilibrium calculations of CO_2/ethanol and CO_2/ethyl acetate mixtures, experimental thermodynamic data (Mehl et al., 2011; Wagner and Pavlíček, 1994) was added to the ASPEN properties database.

2.7. Economic analysis

The economic analysis was performed considering the pre-treatment (drying), extraction, and separation/recovery of solvents steps simultaneously. The analysis followed the Cost of Manufacturing (COM) methodology developed by Turton et al. (2012) and widely applied to SFE processes (Best et al., 2022; Chañi-Paucar et al., 2022; de Melo et al., 2014a; Martins et al., 2016; M.F.F. Rodrigues et al., 2019; V.H. Rodrigues et al., 2019; Zabot et al., 2018). The annual cost of a process (direct and fixed manufacturing costs plus general expenses) is a function of five main components, namely, fixed investment cost (FCI), labor cost (COL), utilities cost (CUT), raw materials cost (CRM), and waste treatment cost (CWT), as described by:

$$COM = 0.304FCI + 2.73COL + 1.23(CUT + CRM + CWT) \quad (4)$$

Besides COM, the more informative values of COM_{ext}, that correspond to the COM divided by the productivity, are also computed since distinct operating conditions impact not only COM but also yields and extracts concentrations.

Regarding the FCI, the base SFE unit consists of 3 × 1 m^3 extractors in parallel, projected to process an amount of *A. dealbata* Link. bark corresponding of 5–10 % of the *E. globulus* Labill. bark generated at a pulp and paper mill located in Aveiro, Portugal (The Navigator Company, 2021). For Process A, the price of the SFE unit was estimated according to the expression proposed by E. Lack for multipurpose SFE units of 3 extractors (it includes the CO_2 pump, storage tank, separator and heating/cooling systems) (Lack et al., 2001). The compressor cost was estimated from a 1 L existing plant (Pereira et al., 2017) and scaled-up using Eq. 5:

$$FCI_2 = FCI_1 \left(\frac{V_2}{V_1}\right)^n \quad (5)$$

where FCI_1 is the cost of a plant of capacity V_1, and FCI_2 is the estimated cost of an equipment with capacity V_2.

Regarding Process B, in addition to all the equipment of Process A, the separator, cosolvent pump and storage tank were all scaled-up from

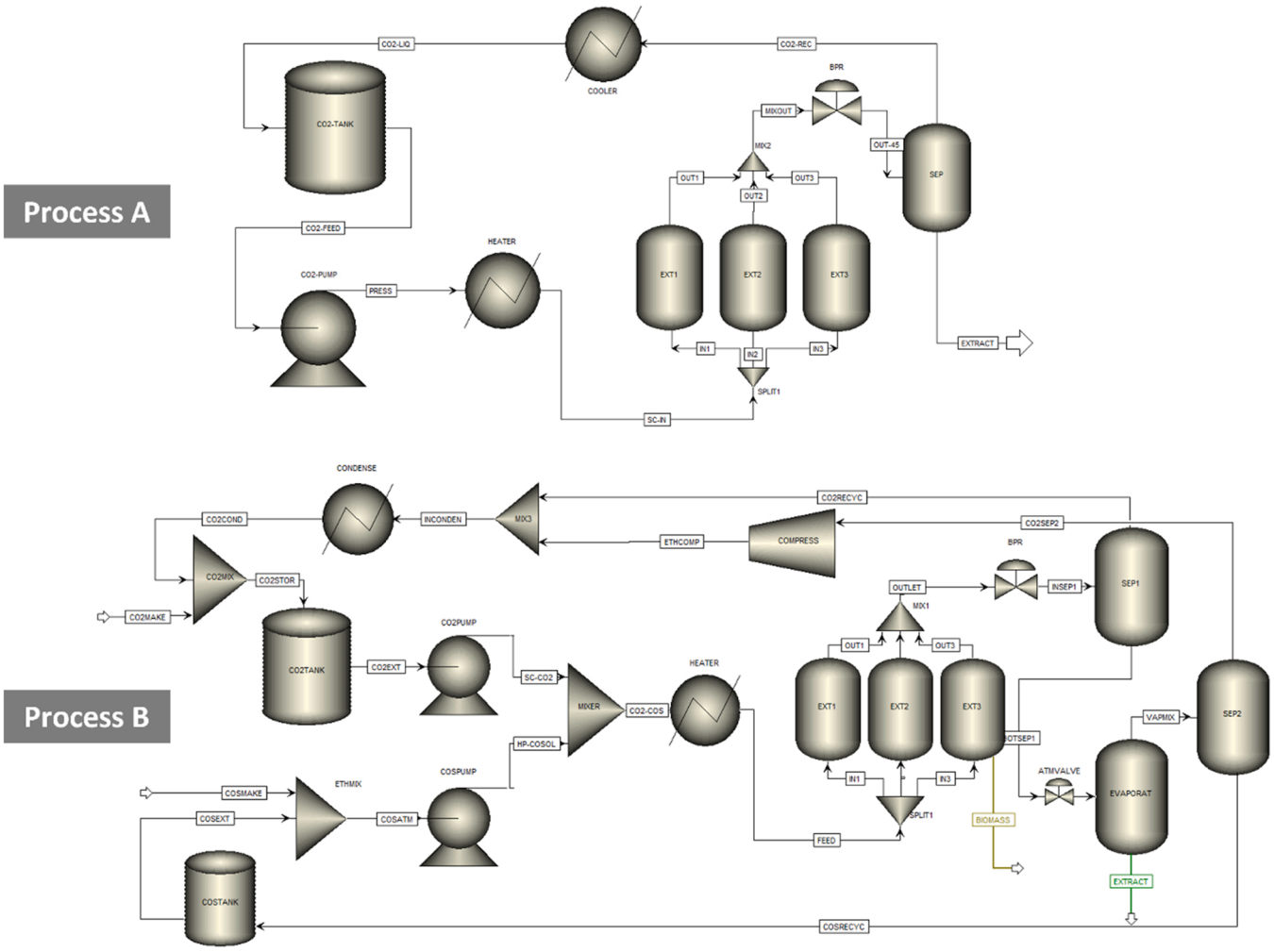

Fig. 1. Diagram of the SFE process simulated in ASPEN plus: Process A - extraction with pure SC-CO_2; Process B - extraction with SC-CO_2 modified with ethanol or ethyl acetate. Retrieved from (V.H. Rodrigues et al., 2019).

a 1 L existing plant (Pereira et al., 2017). The evaporator cost was estimated using the Module Costing Technique (Turton et al., 2012). Furthermore, the addition of flammable cosolvents, such as ethanol and ethyl acetate, requires special precautions such as the use of explosion proof equipment (ATEX Directives). The ATEX factor for Process B was two times the base cost of the equipment. The drying module was not included in the ATEX part of the plant. Every equipment cost estimation was updated using CEPCI index. All the assumptions considered for the determination of COM components are listed in Table 2.

3. Results and Discussion

3.1. Total extraction yield (η_{Total})

The total extraction yields (η_{Total}) determined for the Soxhlet and SFE (with and without cosolvent) assays are presented in Fig. 2. One can see that the reference Soxhlet extraction with dichloromethane scored 1.4 wt% ± 0.05 wt%. This value is lower than those found for the biomass studied in previous works, namely the SFE of a different lot of *A. dealbata* bark (Rodrigues et al., 2021a) and the characterization work on *A. dealbata* biomass (Oliveira et al., 2020), respectively.

For the SFE assays, η_{Total} ranged from 0.06 wt% to 1.57 wt%. The lowest value was obtained with CO_2 modified 5 wt% of ethyl acetate or ethanol, at 10 MPa and 80 °C (runs SFE5_EA and SFE5_EtOH). The highest yield was achieved with 10 wt% of ethanol, at 10 MPa and 60 °C (run SFE9_EtOH). When using pure CO_2 (assays SFE1 - SFE3), the η_{Total} reached 0.66 wt%, 0.58 wt% and 0.44 wt%, obtained at 20 MPa and 80 °C (SFE2), 30 MPa and 60 °C (SFE3), and 20 MPa and 40 °C (SFE1), respectively. These differences can be explained by the effect of pressure, temperature and modifiers added to the SC-CO_2 on the supercritical fluid and solutes properties as discussed in the following.

It is known that the increase of pressure favors the density of the SC-CO_2, increasing its solvent power, as can be observed for runs SFE5 and SFE8 – see Table 1. In fact, at 80 °C, an increase of pressure from 10 M to 30 MPa almost triples the density of CO_2 modified with 5 wt% of ethyl acetate, from 265.29 kg m^{-3} to 764.74 kg m^{-3}, or ethanol, from 254.00 kg m^{-3} to 715.8 kg m^{-3}, and increases η_{Total} by a factor of 18 or 23, from 0.06 wt% to 1.12 wt% and 1.40 wt%, respectively. The effect of increasing temperature is more complex, as it reduces the SC-CO_2 density but it also increases the solutes vapor pressure, thus increasing their solubility. For instance, even though the increase of temperature from 40 °C to 80 °C at 20 MPa (runs SFE1 and SFE2) led to a 29 % decrease of SC-CO_2 density, from 826.20 kg m^{-3} to 586.13 kg m^{-3}, the η_{Total} increased by 50 %, from 0.44 wt% to 0.66 wt%, which shows that the solutes vapour pressure increase outweighed the density decrease. On the contrary, at 10 MPa and with 5 wt% of ethanol or ethyl acetate (runs SFE4 and SFE5) the same increase of temperature decreased the supercritical fluid density by 64 %, from 746.34 kg m^{-3} to 265.29 kg m^{-3}, and 66 %, from 743.64 kg m^{-3} to 254.00 kg m^{-3}, respectively, while the η_{Total} decreased by 84 % and 88 %, from 0.38 wt% and 0.51–0.06 wt %, respectively. In this case the decrease of the supercritical fluid density outweighed the increase of solutes vapour pressure. This change in SC-

Table 2
List of features and assumptions that support the determination of each cost component of COM.

General	Unit working period: 24 h per day; 330 days per year	
	No. of workers per shift:	2
	for extraction times higher than 1 h	
	for extraction times lower than 1 h	3
	Scale-up criterion: Q_{CO_2} w_{bark}^{-1} (kg_{CO_2} h^{-1} kg_{bark}^{-1})	14.4
	Required time to unload, load and pressurize extractor - t_p (h)	1
	Minimum pressure in the separator (MPa)	4.5
	Bed porosity	0.75
	Bed density (kgm^{-3})	356.8
	Biomass initial moisture (seasonal parameter, wt%):	
	winter	0.5
	summer	0.2
	Dried bark heat capacity (kJ kg^{-1} K^{-1}) (Garai et al., 2010)	0.912
FCI	Annual depreciation rate (%)	10
	Price of a 3 × 1 m^3 capacity SFE unit (M€) (Lack et al., 2001)	4.64
	Price of belt drying unit (M€)	0.45
	Price of compressor (k€) (Pereira et al., 2017)	85.8
	Price of cosolvent pump, tank, evaporator, separator (M€) (Pereira et al., 2017; Turton et al., 2012)	1.18
	ATEX factor	2
COL	Labor cost (€ h^{-1} $worker^{-1}$)	10
CUT	Cost of electricity (€ $(MWh)^{-1}$) (Portugal, June 2022)	70
	Cost of steam (€ t^{-1})	20
	Centrifugal pump and compressor efficiencies	75 %
CRM	Cost of CO_2 (€ t^{-1})	250
	Cost of ethanol (€ t^{-1})	1000
	Cost of ethyl acetate (€ t^{-1})	1600
	Cost of bark drying (€ t^{-1})	22
CWT	Cost of waste treatment (€)	0

CO_2 properties becomes more significant closer to the critical region of the fluid, where small changes in pressure and temperature drastically change the fluid properties. This was the case of the previous examples, in which the lower operating pressure did not provide enough solvent density for an efficient extraction at the temperatures tested. As the pressure increases the supercritical fluid is further compressed and allows the use of higher temperatures without compromising the solvent power.

The addition of ethanol or ethyl acetate as cosolvent favored η_{Total}, as can be observed by comparing runs SFE1-SFE3 (light blue bars – pure SC-CO_2) and SFE4-SFE12 (dark blue and green bars – SC-CO_2 modified with ethanol and ethyl acetate, respectively) with the latter attaining higher η_{Total}. This improvement is explained with the modification of CO_2 with solvents of higher polarity, like ethanol and ethyl acetate (dipolar moments of 1.7 D and 1.9 D, respectively (Poling et al., 2001)), targeting a wider range of extractives while impregnating the bark with the cosolvent, improving solutes mass transfer. For instance, the addition of 10 wt% of ethyl acetate or ethanol to the pure SC-CO_2 at 30 MPa and 60 °C (SFE3) improved η_{Total} by 67 % (SFE12_EA) and 100 % (SFE12_EtOH), respectively. A similar increase was observed at 20 MPa and 80 °C, between runs SFE2 (pure CO_2,) and SFE11_EA (10 wt% ethyl acetate) and SFE11_EtOH (10 wt% ethanol). At 20 MPa and 40 °C (SFE1), the addition of 10 wt% of ethyl acetate (SFE10_EA) increased η_{Total} from 0.44 wt% to 0.53 wt%, whereas the addition of 10 wt% of ethanol (SFE10_EtOH) more than doubled the result obtained with pure CO_2.

Surprisingly, at 10 MPa and 60 °C, the maximum η_{Total} (1.57 wt%, SFE9_EtOH) even surpassed that of the Soxhlet with dichloromethane (1.40 wt%). At this pressure and temperature the SC-CO_2 density is low (304.75 kg m^{-3}) but it increases significantly when modified with 10 wt % of ethyl acetate or ethanol to 630.02 kg m^{-3} and 640.34 kg m^{-3}, respectively, but so does the critical point of the mixture when modified with 10 wt% ethanol, *ca.* 9.6 MPa and 51 °C (estimated from experimental data (Baker and Anderson, 1957; Lim et al., 1994; Takishima et al., 1986; Yeo et al., 2000)). It is fundamental to report that, at the end of run SFE9_EtOH, it was verified that the biomass was wet and there was accumulation of liquid ethanol during the extraction. This accumulation swells the bark matrix and may have contributed to the solutes solubilisation (in the unbound ethanol *moisture*), enhancing their transport to the biomass surface, after which they are extracted by convection to the supercritical fluid bulk. According to this hypothesis, the extraction may globally combine two mechanisms in parallel: (i) a solid-SCF extraction, *i.e.* the conventional SFE; (ii) a two steps in series

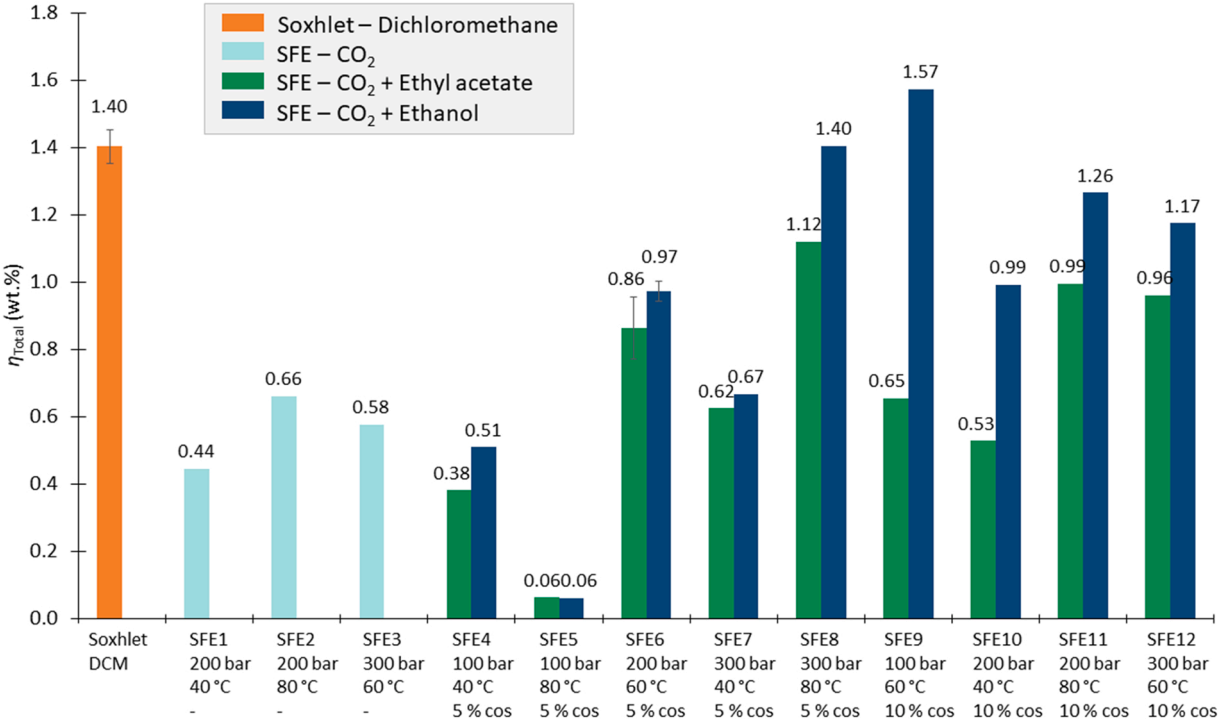

Fig. 2. Total extraction yields (η_{Total}) obtained by Soxhlet using dichloromethane (DCM) and SFE with ethanol and ethyl acetate as cosolvents. Error bars correspond to assays performed in triplicate. See Table 1.

process, *i.e.* a solid-liquid extraction in the porous biomass (solutes solubilization and intraparticle diffusion) followed by a liquid-SCF extraction. Notwithstanding the higher diffusivities in supercritical solvents in comparison with liquids, the second mechanism takes advantage of the increment of the mass transfer driving force associated with the higher solutes concentration inside the particle.

Overall, the increase of pressure, temperature and addition of cosolvents favoured the η_{Total}, specially in the modification with ethanol, reaching the value of the Soxhlet extraction with dichloromethane. In terms of variability, the modification with ethyl acetate shows greater standard deviations than with ethanol, as can be observed in the error bars of runs SFE6_EA and SFE6_EtOH.

3.2. Lupenyl acetate and lupenone yields

Total extraction yield results may give a blind insight on process productivity, but it is its combination with the desired compounds individual yields that determines the process yield for a given molecule. The individual extraction yields of lupenyl acetate (LA) and lupenone (Lu), the main triterpenoids extracted from the bark of *A. dealbata* Link., are presented in Fig. 3. At first, one may notice that the extraction yields of both compounds in most runs surpassed those obtained by Soxhlet with dichloromethane, 347.4 mg kg_{bark}^{-1} and 269.7 mg kg_{bark}^{-1} for LA and Lu, respectively, ranging from 22.7 mg kg_{bark}^{-1} to 777.5 mg kg_{bark}^{-1} for LA and from 13.5 mg kg_{bark}^{-1} to 679.8 mg kg_{bark}^{-1} for Lu. Unlike for η_{Total}, one may say that the yields of LA and Lu using pure SC-CO_2 have an identical range with those obtained with modified SC-CO_2, given the error bars presented in runs SFE6_EA and SFE6_EtOH. Furthermore, it becomes clear that even though ethanol was more favorable for η_{Total}, it produced lower individual extraction yields of LA and Lu.

The differences between runs can be explained with the changes in the experimental conditions. For instance, the effect of pressure and temperature can be observed between runs SFE2 (20 MPa, 80 °C) and SFE1 (20 MPa, 40 °C), where only pure CO_2 was used. When temperature was reduced by 40 °C, density increased from 586.13 kg m^{-3} to 826.20 kg m^{-3} resulting in higher yields of LA and Lu (increase of 54 % and 69 %, respectively). However, when run SFE3 (30 MPa, 60 °C) is compared with SFE1 (20 MPa, 40 °C), the density does not change significantly from SFE1, even though a similar drop in the LA and Lu yields is observed. This result indicates that higher temperatures may not favor the yields of LA and Lu over the (20−30) MPa pressure range. On the contrary, the addition of ethyl acetate and ethanol as cosolvents provided the highest individual yields of LA (777.5 mg kg_{bark}^{-1} and 589.5 mg kg_{bark}^{-1}) at the highest temperature, namely in runs SFE11_EA (20 MPa, 80 °C, 10 wt% ethyl acetate) and SFE8_EtOH (30 MPa, 80 °C, 5 wt% ethanol), respectively. Runs SFE5 (10 MPa, 80 °C, 5 wt% cosolvent) produced very small amounts of both compounds regardless of the cosolvent, as could be predicted by the low η_{Total}. In the case of runs SFE9 (10 MPa, 60 °C, 10 wt% cosolvent), which were previously discussed due to the proximity to the critical point and due to cosolvent accumulation during extraction, no unexpected result was observed for the two compounds yields, especially with ethanol, taking into consideration it achieved the highest η_{Total}.

In general, the effect of pressure, temperature and cosolvents addition was not pronounced and showed that despite the significant changes observed for η_{Total}, LA and Lu yields did not follow a clear trend.

3.3. Lupenyl acetate and lupenone contents

Total and individual extraction yields indicate the potential of SFE in terms of whole extract and individual compounds productivity. Nonetheless, to infer the selectivity of the process and the best experimental conditions to obtain the desired compounds, the extracts concentrations of LA and Lu were determined. The results can be observed in Fig. 4.

The concentrations of LA and Lu in the Soxhlet extracts scored 2.4 wt % and 1.9 wt%, respectively. These values are lower than those obtained by SFE, which ranged from 2.0 wt% to 15.8 wt% for LA (SFE9_EtOH and SFE4_EA) and from 1.5 wt% to 12.8 wt% for Lu (SFE9_EtOH and SFE1). In contrast with what was observed for the total and individual extraction yields (Fig. 2 and Fig. 3), the range of concentrations of LA and Lu obtained with pure SC-CO_2, (6.7–15.4) wt% and (5.0–12.8) wt%,

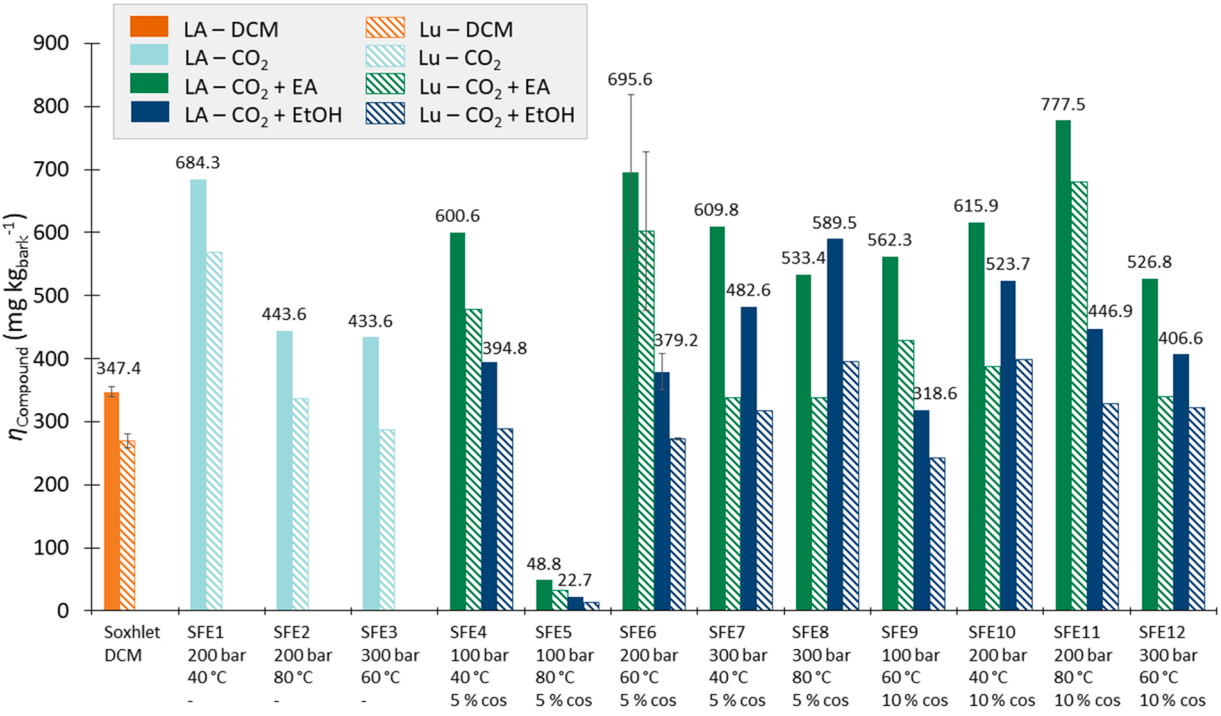

Fig. 3. Lupenyl acetate (LA) and lupenone (Lu) yields in the extract obtained with Soxhlet using dichloromethane and SFE with pure CO_2 and with ethanol and ethyl acetate as cosolvents. Errors bars correspond to assays performed in triplicate. See Table 1.

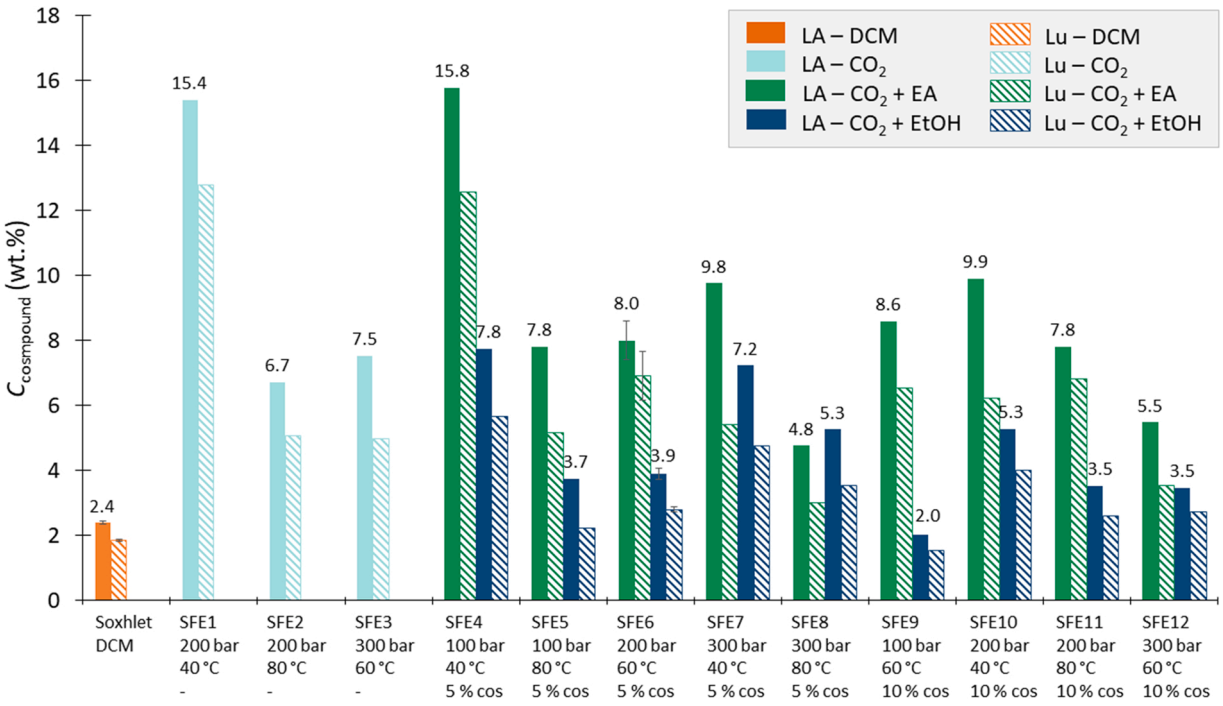

Fig. 4. Lupenyl acetate (LA) and lupenone (Lu) concentrations in the extract obtained with Soxhlet using dichloromethane (DCM) and SFE with pure CO_2 and with ethanol and ethyl acetate as cosolvents. Errors bars correspond to assays performed in triplicate. See Table 1.

respectively, were identical with the ones observed when using ethyl acetate as cosolvent, (4.8–15.8) wt%, and (3.0–12.6) wt%, respectively, and higher than those obtained with the addition of ethanol, (2.0–7.8) wt% and (1.5–5.7) wt%, respectively. These values show that Soxhlet extraction and SFE most productive conditions are not accompanied with a higher concentration of the desired compounds, as a result of dilution in a wider extract. On the contrary, the less productive SFE conditions present higher selectivities for the two compounds. This can be observed in runs SFE4_EA and SFE10_EA, using ethyl acetate as cosolvent, where η_{Total} was 0.38 wt% and 0.53 wt%, respectively, but LA concentrations were the highest (15.8 wt% and 9.9 wt%, respectively). The same is verified for the runs with ethanol, namely SFE4_EtOH and SFE7_EtOH, where η_{Total} scored 0.51 wt% and 0.67 wt%, respectively, while the two highest LA concentrations in ethanol modified runs scored 7.8 wt% and 7.2 wt%, respectively. Pure SC-CO_2 assays follow the same trend, with η_{Total} of 0.44 wt%, 0.58 wt% and 0.67 wt% corresponding to LA concentrations of 15.4 wt%, 7.5 wt% and 6.7 wt%, runs SFE1, SFE3 and SFE2, respectively. The case of run SFE9_EtOH is another example of the previous observation as it showed the highest η_{Total} (1.57 wt%) and the lowest concentration of LA (2.0 wt%).

Overall, the best concentrations of both LA and Lu were observed in the region of medium to low temperature and pressure, for pure and modified SC-CO_2, even though pure SC-CO_2 and the modification with ethyl acetate gave the best results. Based on these results, seven runs were selected for a preliminary economic evaluation, namely SFE1, SFE2 and SFE3 all using pure SC-CO_2, and SFE4_EtOH, SFE8_EtOH, SFE4_EA and SFE8_EA all using SC-CO_2 modified with 5 wt% of ethanol or ethyl acetate as cosolvent. This selection intends to evaluate the effect of pressure and temperature on the economics of the process, as well as compare the results of pure SC-CO_2 process with a modified SC-CO_2 plant at conditions focusing productivity or selectivity towards LA and Lu.

3.4. Supercritical fluid extraction curves

Two SFE curves were measured under the optima conditions identified in previous sections towards triterpenoids yield and concentrations (20 MPa and 40 °C). To assess the influence of mass flow rate, these experiments were carried out at 12 and 18 g min^{-1}, corresponding to solvent to feed mass ratios of 86.4 kg kg^{-1} and 129.6 kg kg^{-1} at the end of the extraction (6 h), runs SFE1_C1 and SFE1_C2, respectively (see Fig. 5A). The final total extraction yields of the two SFE curves are very similar, η_{Total} = 0.42wt.% (SFE1_C1) and 0.45 wt% (SFE1_C2) and agree with run SFE1 (0.44 wt%). Nonetheless, an important difference between those two curves can be observed during the first half hour of

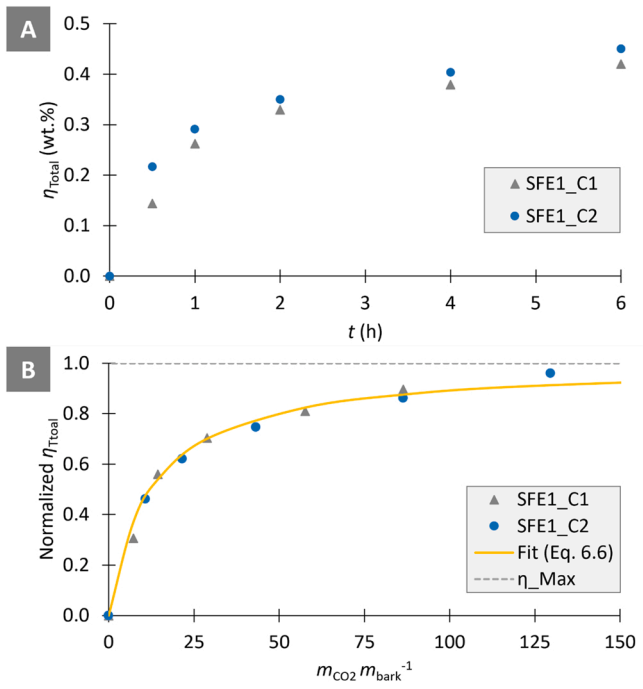

Fig. 5. SFE curves of *A. dealbata*. bark: A – total extraction yield *versus* time; B – normalized total extraction yield as function of the mass of spent CO_2 per unit mass of bark.

extraction, for which run SFE1_C2 exhibits a higher extraction rate than SFE1_C1, while for the remaining extraction time they become identical. These results suggest that increasing CO_2 flow rate above 12 g min^{-1} (*i.e.*,14.4 kg_{CO2} h^{-1} kg_{bark}^{-1}) does not significantly improve the extraction performance, and it is counter-productive taking into account the additional energy costs and spent CO_2. A similar result was observed for the SFE of *E. globulus* Labill bark using solvent flow rate to feed mass ratios higher than 60 kg_{CO2} kg_{bark}^{-1} (Domingues et al., 2012a), a value that was validated with a scale-up study at 10 and 100 times the laboratory scale (de Melo et al., 2014b).

When the two $\eta_{Total}(t)$ curves (SFE1_C1 and SFE1_C2) are normalized by the maximum yield ($\eta_{Total,max}$ obtained by fitting Eq. (6) to data) and plotted as function of the solvent to feed mass ratio ($m_{CO_2} m_{bark}^{-1}$), they fall into a single curve as shown in Fig. 5B.

$$\frac{\eta_{Total}}{\eta_{Total,max}} = \frac{K \quad m_{CO_2} m_{bark}^{-1}}{1 + K \quad m_{CO_2} m_{bark}^{-1}} \tag{6}$$

where K and $\eta_{Total,max}$ are fitting parameters.

A similar analysis was accomplished for SFE curves of *E. globulus* Labill. bark, measured at several operating conditions. A set of four extraction curves taken from the literature is listed in Table 3, comprising assays carried out at 20 MPa and 40 °C or 60 °C, with SC-CO_2 modified with (0–5) wt% ethanol, CO_2 flow rates in the range (6–12) g min^{-1}, and total extraction times of (6.0–6.5) h. When the experimental results are plotted under the same coordinates of Fig. 5B (*i.e.,* normalized yield against $m_{CO_2} m_{bark}^{-1}$), the four curves overlap into a common curve, independently of the employment of cosolvent, solvent flow rate and temperature (see Fig. 6). Such overlap may be attributed to compensating effects of the process variables upon the extraction behavior, which means that in the studied ranges of operating conditions the mass of spent CO_2 per unit mass of bark can be seen as the relevant lumped variable. However, the detailed analysis of each variable upon the extraction yield is provided in the original references (de Melo et al., 2014b; Domingues et al., 2012a; V.H. Rodrigues et al., 2019).

3.5. Economic analysis

The influence of pressure, temperature and cosolvents addition on the economics of the process was evaluated using the 21 final point experiments of Table 1, namely: SFE#, SFE_EA# and SFE_EtOH#. The first step is the determination of the best extraction time (or best mass of spent CO_2).

It is frequently found that the most productive period in the case of the SFE of biomasses usually occurs during the first two hours of extraction, more precisely in the transition between the extraction periods governed by external and internal mass transfer limitations. The optimum extraction time or mass of spent CO_2 is determined, as a first approximation, by intersecting the tangential lines characteristic of each period (de Melo et al., 2014a; V.H. Rodrigues et al., 2019).

Based on the superimposed extraction curves of *A. dealbata* Link. bark obtained at 20 MPa, 40 °C, and (12 and 18) g min^{-1} of SC-CO_2 (see Fig. 5B), the optimum abscissa was determined intersecting the maximum normalized yield ($\eta_{Total}/\eta_{Total,max} = 1$) with the initial linear period of constant extraction rate (CER) as shown in Fig. 7. Such

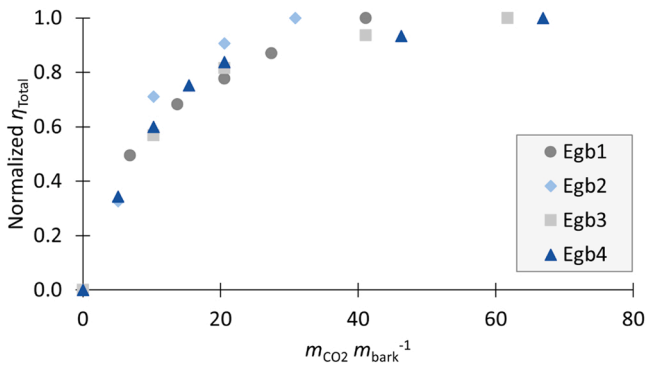

Fig. 6. Normalized η_{Total} SFE curves of *E. globulus* Labill. bark as function of the mass of spent CO_2 per unit mass of bark.

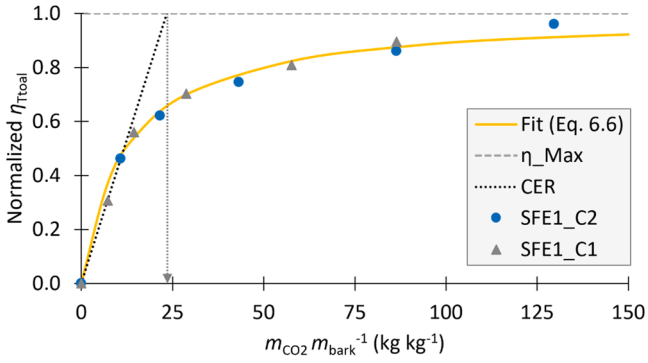

Fig. 7. Normalized η_{Total} curve fitted (Eq. (6)) to the two *A. dealbata* Link. SFE extraction curves. The two asymptotic periods of extraction were fitted with linear functions. The intersection of both lines identifies the optimum ratio of spent mass of CO_2 to mass of bark.

optimum occurs at $m_{CO_2} m_{bark}^{-1}$ = 23.4 kg kg^{-1}, and corresponds to $\eta_{Total}/\eta_{Total,max}$ = 65.5%. Considering the pseudo-universal curve also observed for the SFE of *E. globulus* Labill. bark (Fig. 6), this optimum will be settled independently of cosolvent utilization. Since the CO_2 mass flow rate and the mass of bark are fixed for the abovementioned 21 final point experiments, the corresponding optimum time is 1.63 h. This confirms that the optimum extraction time is much lower than the 6 h of the kinetic experiments for which the mass ratios were 86.4 kg kg^{-1} and 129.6 kg kg^{-1}, which translates in a significant decrease of the spent CO_2 down to 23.4 kg kg^{-1} at higher scales. This value will be further refined in the following.

In the following paragraphs a COM analysis will be carried out for several scenarios, using the same optimized condition as a first approximation. Taking into account that different operating conditions give rise to distinct yields, different COM values result due to changes in density, solubility of solutes, among others. However, the calculated COM_{ext} will emphasize the influence of productivity, *i.e.* of the various associated yields.

Seven scenarios were selected for the economic evaluation (SFE1,

Table 3
List of SFE curves retrieved from the literature for *Eucalyptus globulus* Labill. bark under different conditions of pressure, temperature, cosolvent content, and ratio of SC-CO_2 mass flow rate to bark weight.

# Run	Morphological part	P (MPa)	T (°C)	Ethanol content (wt%)	$Q_{CO_2} m_{bark}^{-1}$ (kg h^{-1} kg^{-1})	Ref.
Egb1	Bark	20	60	0	6.9	(V.H. Rodrigues et al., 2019)
Egb2	Bark	20	40	2.5	10	(de Melo et al., 2014b)
Egb3	Bark	20	40	5	5	(Domingues et al., 2012a)
Egb4	Bark	20	40	5	10	(Domingues et al., 2012a)

Table 4
Results of the preliminary economic evaluation of the seven scenarios in terms of η_{Total}, productivity, COM and COM_{ext}, calculated for the optimum extraction time of 1.63 h (see Fig. 7).

Run	η_{Total} (wt.%)	Productivity (t_{year}^{-1})	COM (M€)	COM_{ext} ($€kg_{extract}^{-1}$)
SFE1	0.29	9.4	1.26	134.0
SFE2	0.43	14.0	1.26	90.3
SFE3	0.38	12.2	1.28	104.9
SFE4_EtOH	0.33	10.7	1.75	163.3
SFE8_EtOH	0.92	29.6	1.79	60.5
SFE4_EA	0.25	8.0	1.72	213.8
SFE8_EA	0.73	23.6	1.75	74.1

SFE2, SFE3, SFE4_EA, SFE8_EA, SFE4_EtOH and SFE8_EtOH), compiled in Table 4 along with the values of η_{Total}, productivity, COM, and COM_{ext} (remember it corresponds to COM divided by productivity) for the optimum time of 1.63 h. For all seven scenarios, the amount of *A. dealbata* Link. bark processed annually corresponds to 3223.4 t. One can see that the COM results are similar for the runs with pure SC-CO_2, showing that the effect of the different pressures and temperatures led to COM values that differ less than 1 %. The major differences occur between pure and modified CO_2 runs, which are mainly due to the higher equipment cost of Process B. If the analysis is focused solely on the COM value, any of the runs using Process A (SFE1-SFE3) seems favorable since the annual cost is at least 26 % lower than for Process B. However, when the productivity is taken into account, the process and operating conditions have a significant effect on COM_{ext}, ranging from 60.5 $€kg_{extract}^{-1}$ to 213.8 $€kg_{extract}^{-1}$, corresponding to the highest and lowest productivities, (29.6 and 8.0) t y^{-1}, obtained in runs SFE8_EtOH and SFE4_EA, respectively. Nonetheless, it is worth noting that for smaller changes in productivity the additional costs of employing cosolvents can outweigh the productivity gain, as can be observed between runs SFE1 and SFE4_EtOH. Even though SFE1 produced less extract (9.4 *versus* 10.7) t $year^{-1}$, the COM_{ext} was still lower (134 *versus* 163.3) $€kg_{extract}^{-1}$.

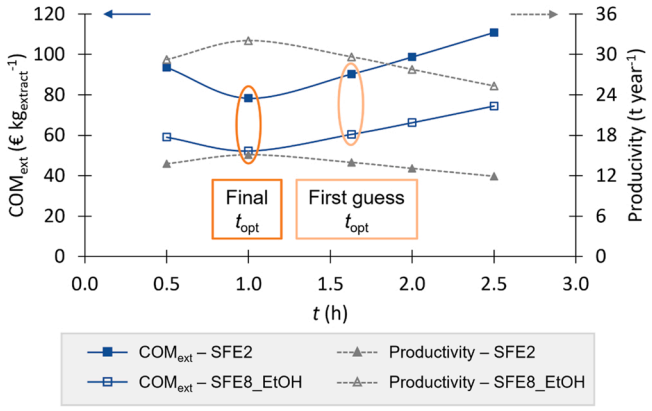

Fig. 8. Effect of extraction time on COM_{ext} (left ordinate) and productivity (right ordinate) for runs SFE2 and SFE8_EtOH. The first guess and final value of the optimum extraction time (t_{opt}) are highlighted.

From an economic perspective, run SFE2 seems the most favourable of the three pure SC-CO_2 runs, especially when compared with SFE1 as COM_{ext} is 90.3 $€kg_{extract}^{-1}$ against 134.0 $€kg_{extract}^{-1}$, respectively. Nonetheless, it is important to remind that these two runs obtained significantly different triterpenoids concentrations, 15.4 wt% and 6.7 wt% for SFE1 and SFE2, respectively (see Fig. 4), which means that if the triterpenoids purity in the extract is the target response a more expensive operating condition is preferable. In comparison with the previous economic analysis of the SFE of *E. globulus* Labill. bark, which achieved a minimum COM_{ext} of 28.1 $€kg_{extract}^{-1}$ (Rodrigues et al., 2019; V.H. Rodrigues et al., 2019), the current value for acacia is much higher. However, it is worth noting such low COM_{ext} was obtained for an industrial *E. globulus* plant.

The effect of the extraction time on COM_{ext} of runs SFE2 and SFE8_EtOH was evaluated in more detail from 0.5 h to 2.5 h, as shown in Fig. 8, taking into account the intersection method illustrated in Fig. 7 is appropriate to generate first guesses.

It is possible to see that the optimum extraction time determined before (1.63 h) does not correspond to the minimum COM_{ext}, which is further reduced for extraction times as low as 1 h, reaching 78.3 $€kg_{extract}^{-1}$ and 52.3 $€kg_{extract}^{-1}$, a decrease of 13 % and 14 % for runs SFE2 and SFE8_EtOH, respectively. This result is explained by approaching the initial period of extraction, where the extraction rate and productivity are maximized (see Fig. 7), though higher annual amounts of bark are processed (32 % higher, specifically 4239 t). Moreover, in the case of extraction times lower than 1 h (time required to unload, load, and pressurize the extractor), the labor demand increases and an additional employee per shift was considered in the simulations (see Table 2), which increased COM_{ext} significantly.

Based on the best COM_{ext} scenarios for pure and modified CO_2 (SFE2 and SFE8_EtOH, respectively), the distributions of the COM_{ext} components were analyzed and can be visualized in Fig. 9. Here, one can see that the SC-CO_2 process modified with 5 wt% ethanol has higher FCI and CRM fractions, balanced by the decrease of COL and CUT fractions. Among the four fractions, CUT represents almost half of the costs followed by COL, which varies from around one quarter to one third of the COM. Even though variations of each COM_{ext} parcel were already discussed, it is important to note that these were influenced by the productivity. For instance, while the addition of 5 wt% ethanol increased the FCI fraction by 69 %, the real increase of the investment cost (CAPEX) was from 5.2 M€ to 12.3 M€, which corresponds to an increase

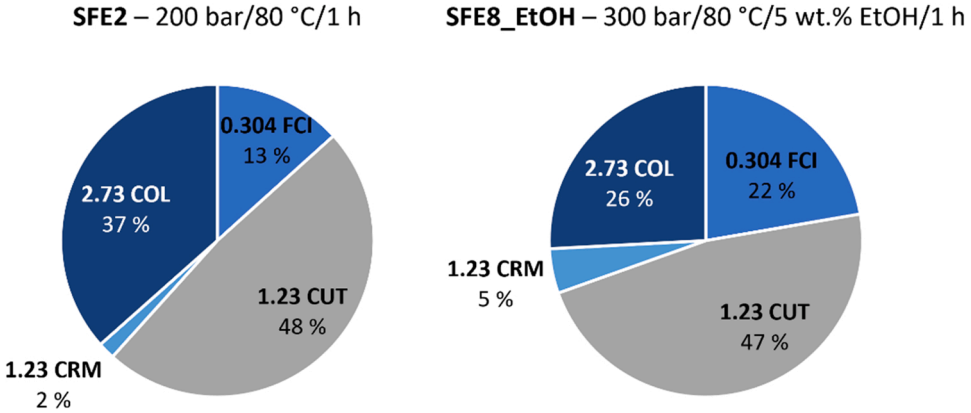

Fig. 9. Pie charts of the COM_{ext} components distribution for runs SFE2 (left) and SFE8_EtOH (right).

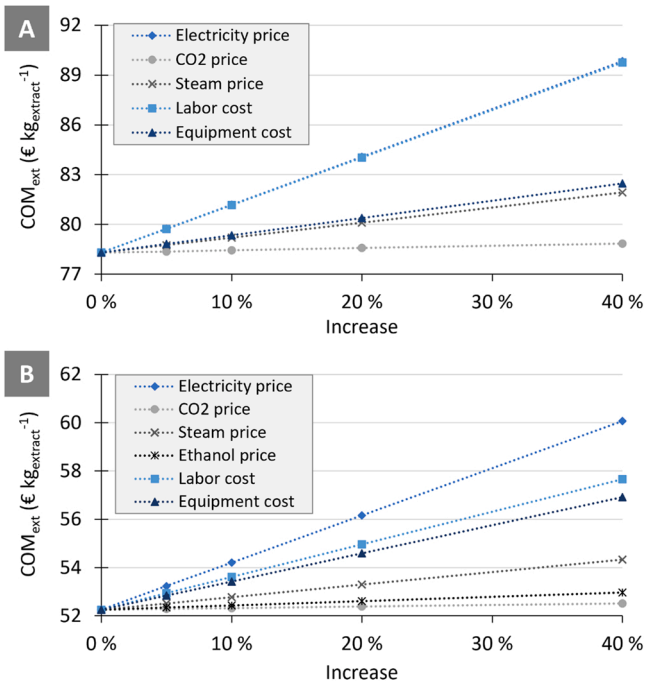

Fig. 10. Sensitivity analysis plot. Effect of the increase of the costs of utilities, raw materials, labor, and equipment on the COM_{ext} for the two scenarios considered using an optimum extraction time of 1 h: A – SFE2; B -SFE8_EtOH.

of 137 %, while the operating costs (OPEX) increased from 1.0 M€ to 1.3 M€, a 27 % increase.

The low fraction of CRM of the total costs (2 % and 5 %; see Fig. 9) can be attributed to the addition of a compressor to recover the CO_2 lost between extraction cycles, as well as the extra equipment included for the cosolvent recovery. If the recompression (from a minimum pressure of 0.5 MPa) of the CO_2 lost between extraction cycles had not been considered, the final COM_{ext} for SFE2 and SFE8_EtOH would increase to 90.6 $€kg_{extract}^{-1}$ and 58.0 $€kg_{extract}^{-1}$, respectively, demonstrating the importance of an efficient management of raw materials.

A sensitivity analysis was performed varying the values of several economic parameters (electricity and steam prices, CO_2 and ethanol prices, and the labor and equipment costs) and calculating their impact on the estimated COM_{ext} (see Fig. 10). In all cases the most rigorous optimum extraction time of 1 h was considered. As can be observed, for an increase of 5–40 %, the electricity price is the variable with the highest impact on COM_{ext} for both runs SFE2 and SFE8_EtOH, respectively. In the case of SFE2, the increase of the electricity price and labor cost showed a similar effect on COM_{ext} (runs overlapped in Fig. 10A), while the remaining variables did not raise the COM_{ext} value by more than 5.3 %. Regarding SFE8_EtOH (Fig. 10B), the labor cost was also the second most influent variable, followed by the equipment cost, whereas the steam, CO_2 and ethanol prices did not increase COM_{ext} by more than 4.0 %. These results agree with the analysis of the COM_{ext} components distribution (Fig. 9) and provide further details on the effect of several variables costs assumed during this work.

4. Conclusions

The increase of pressure, temperature and cosolvent content favoured η_{Total}, which reached a maximum of 1.57 wt%. The most selective operating conditions were 20 MPa and 40 °C without cosolvents, reaching the Soxhlet η_{Total}, whereas the LA yields and concentrations were more than two and six times higher than those of the conventional extraction method, respectively. The addition of ethyl acetate and ethanol improved the productivity, η_{Total}, but the lupane triterpenoids yields and concentrations were similar or lower than with pure SC-CO_2.

The effect of the CO_2 mass flow rate was studied with two kinetic extraction curves. Based on the similar pace of the normalized η_{Total} SFE curves as function of the ratio $m_{CO_2} m_{bark}^{-1}$, the optimum extraction time for SFE of acacia bark was estimated by the intersection method to be 1.63 h (or 23.4 $kg_{CO_2} kg_{bark}^{-1}$). Subsequently, this value was rigorously analyzed giving rise to $t_{opt} = 1$ h, for which the lowest COM_{ext} were 78.3 $€kg_{extract}^{-1}$ for pure SC-CO_2 (at 20 MPa and 80 °C), and 52.3 $€kg_{extract}^{-1}$ for SC-CO_2 modified with 5 wt% ethanol (at 30 MPa and 80 °C). Hence, the economic analysis revealed that the addition of ethanol is economically advantageous due to the higher productivities, despite the higher investment costs associated. In contrast, the more selective conditions to obtain LA and Lu showed higher COM_{ext}. In the whole, the major contributor for the costs of both processes were the electricity price and the labor cost.

Overall, this work provides key information for the valorization of *A. dealbata* Link. bark by SFE in terms of extracts productivity and composition, as well as preliminary economic indicators.

CRediT authorship contribution statement

Vítor H. Rodrigues: Writing – original draft, Investigation, Methodology. **Inês Portugal:** Supervision, Writing – review & editing, Formal analysis. **Carlos M. Silva:** Funding acquisition, Supervision, Writing – review & editing, Conceptualization, Resources, Formal analysis.

Declaration of Competing Interest

The authors declare that they have no known competing financial interests or personal relationships that could have appeared to influence the work reported in this paper.

Data Availability

Data will be made available on request.

Acknowledgements

This work was developed within the scope of the project CICECO-Aveiro Institute of Materials, UIDB/50011/2020, UIDP/50011/2020 & LA/P/0006/2020, financed by national funds through the FCT/MCTES (PIDDAC). Authors want to thank Project inpactus—innovative products and technologies from eucalyptus, Project N° 21874 funded by Portugal 2020 through European Regional Development Fund (ERDF) in the frame of COMPETE 2020nº246/AXIS II/2017.

References

Baker, L.C.W., Anderson, T.F., 1957. Some phase relationships in the three-component liquid system CO_2-H_2O-C_2H_5OH at high pressures. J. Am. Chem. Soc. 79, 2071–2074. https://doi.org/10.1021/ja01566a013.

Best, I., Cartagena-Gonzales, Z., Arana-Copa, O., Olivera-Montenegro, L., Zabot, G., 2022. Production of oil and phenolic-rich extracts from mauritia flexuosa l.f. using sequential supercritical and conventional solvent extraction: experimental and economic evaluation. Processes 10 (2022). https://doi.org/10.3390/PR10030459 (459 10, 459).

Casas, M.P., López-Hortas, L., Díaz-Reinoso, B., Moure, A., Domínguez, H., 2021. Supercritical CO_2 extracts from *Acacia dealbata* flowers. J. Supercrit. Fluids 173, 105223. https://doi.org/10.1016/J.SUPFLU.2021.105223.

Cerasoli, S., Caldeira, M.C., Pereira, J.S., Caudullo, G., de Rigo, D., 2016. *Eucalyptus globulus* and other eucalypts in Europe: distribution, habitat, usage and threats. Eur. Atlas For. Tree Species 90–91.

Chañi-Paucar, L.O., Johner, J.C.F., Zabot, G.L., Meireles, M.A.A., 2022. Technical and economic evaluation of supercritical CO_2 extraction of oil from sucupira branca seeds. J. Supercrit. Fluids 181. https://doi.org/10.1016/J.SUPFLU.2021.105494.

Correia, R., Quintela, J.C., Duarte, M.P., Gonçalves, M., 2020. Insights for the valorization of biomass from portuguese invasive acacia spp. in a biorefinery perspective. Forest 11 (2020). https://doi.org/10.3390/F11121342 (1342 11, 1342).

de Melo, M.M.R., Oliveira, E.L.G., Silvestre, A.J.D., Silva, C.M., 2012. Supercritical fluid extraction of triterpenic acids from *Eucalyptus globulus* bark. J. Supercrit. Fluids 70, 137–145. https://doi.org/10.1016/j.supflu.2012.06.017.

de Melo, M.M.R., Domingues, R.M. a, Silvestre, A.J.D., Silva, C.M., 2014. Extraction and purification of triterpenoids using supercritical fluids: from lab to exploitation. Mini-Rev. Org. Chem. 362–381. https://doi.org/10.2174/1570193X113106660002.

de Melo, M.M.R., Barbosa, H.M.A., Passos, C.P., Silva, C.M., 2014a. Supercritical fluid extraction of spent coffee grounds: measurement of extraction curves, oil characterization and economic analysis. J. Supercrit. Fluids 86, 150–159. https://doi.org/10.1016/j.supflu.2013.12.016.

de Melo, M.M.R., Domingues, R.M.A., Sova, M., Lack, E., Seidlitz, H., Lang Jr., F., Silvestre, A.J.D., Silva, C.M., 2014b. Scale-up studies of the supercritical fluid extraction of triterpenic acids from *Eucalyptus globulus* bark. J. Supercrit. Fluids 95, 44–50. https://doi.org/10.1016/j.supflu.2014.07.030.

de Melo, M.M.R., Silvestre, A.J.D., Silva, C.M., 2014c. Supercritical fluid extraction of vegetable matrices: applications, trends and future perspectives of a convincing green technology. J. Supercrit. Fluids 92, 115–176. https://doi.org/10.1016/j.supflu.2014.04.007.

de Melo, M.M.R., Portugal, I., Silvestre, A.J.D., Silva, C.M., 2017. Environmentally benign supercritical fluid extraction. In: Pena-Pereira, F., Tobiszewski, M. (Eds.), The Application of Green Solvents in Separation Processes. Elsevier, pp. 325–348.

de Melo, M.M.R., Carius, B., Simões, M.M.Q., Portugal, I., Saraiva, J., Silva, C.M., 2020. Supercritical CO_2 extraction of *V. vinifera* leaves: influence of cosolvents and particle size on removal kinetics and selectivity to target compounds. J. Supercrit. Fluids 165, 104959. https://doi.org/10.1016/j.supflu.2020.104959.

Domingues, R.M.A., de Melo, M.M.R., Neto, C.P., Silvestre, A.J.D., Silva, C.M., 2012a. Measurement and modeling of supercritical fluid extraction curves of *Eucalyptus globulus* bark: influence of the operating conditions upon yields and extract composition. J. Supercrit. Fluids 72, 176–185. https://doi.org/10.1016/j.supflu.2012.08.010.

Domingues, R.M.A., Oliveira, E.L.G., Freire, C.S.R., Couto, R.M., Simões, P.C., Neto, C.P., Silvestre, A.J.D., Silva, C.M., 2012b. Supercritical fluid extraction of *Eucalyptus globulus* bark-A promising approach for triterpenoid production. Int. J. Mol. Sci. 13, 7648–7662. https://doi.org/10.3390/ijms13067648.

Domingues, R.M.A., de Melo, M.M.R., Oliveira, E.L.G., Neto, C.P., Silvestre, A.J.D., Silva, C.M., 2013. Optimization of the supercritical fluid extraction of triterpenic acids from *Eucalyptus globulus* bark using experimental design. J. Supercrit. Fluids 74, 105–114. https://doi.org/10.1016/j.supflu.2012.12.005.

Falco, N., Kiran, E., 2012. Volumetric properties of ethyl acetate + carbon dioxide binary fluid mixtures at high pressures. J. Supercrit. Fluids 61, 9–24. https://doi.org/10.1016/j.supflu.2011.09.016.

Fereira, A.F., 2017. Biorefinery concept. In: Rabaçal, M., Ferreira, A.F., Silva, C.A.M., Costa, M. (Eds.), Biorefineries - Targeting Energy, High Value Products and Waste Valorisation, Lecture Notes in Energy. Springer International Publishing, Cham. https://doi.org/10.1007/978-3-319-48288-0.

Garai, A., Kleissl, J., Llewellyn Smith, S.G., 2010. Estimation of biomass heat storage using thermal infrared imagery: application to a walnut orchard. Bound.-Layer. Meteor. 137, 333–342. https://doi.org/10.1007/s10546-010-9524-x.

Gross, J., Sadowski, G., 2002. Application of the perturbed-chain SAFT equation of state to associating systems. Ind. Eng. Chem. Res. 41, 5510–5515. https://doi.org/10.1021/ie010954d.

Lack, E., Gamse, T., Marr, R., 2001. Separation operations and equipment. In: Bertucco, A., Vetter, G. (Eds.), High Pressure Technology Fundamentals and Applications. Elsevier, Amsterdam.

Lim, J.S., Lee, Y.Y., Chun, H.S., 1994. Phase equilibria for carbon dioxide-ethanol-water system at elevated pressures. J. Supercrit. Fluids 7, 219–230. https://doi.org/10.1016/0896-8446(94)90009-4.

López-Hortas, L., Rodríguez-González, I., Díaz-Reinoso, B., Torres, M.D., Moure, A., Domínguez, H., 2021. Tools for a multiproduct biorefinery of *Acacia dealbata* biomass. Ind. Crops Prod. 169, 113655 https://doi.org/10.1016/J.INDCROP.2021.113655.

Lucetti, D.L., Lucetti, E.C.P., Bandeira, M., Veras, H.N.H., Silva, A.H., Leal, L., Lopes, A.A., Alves, V.C.C., Silva, G.S., Brito, G., Viana, G.B., 2010. Anti-inflammatory effects and possible mechanism of action of lupeol acetate isolated from *Himatanthus drasticus* (Mart.) Plumel. J. Inflamm. 7, 60. https://doi.org/10.1186/1476-9255-7-60.

Martins, P.F., de Melo, M.M.R., Silva, C.M., 2016. Techno-economic optimization of the subcritical fluid extraction of oil from *Moringa oleifera* seeds and subsequent production of a purified sterols fraction. J. Supercrit. Fluids 107, 682–689. https://doi.org/10.1016/j.supflu.2015.07.031.

Mehl, A., Nascimento, F.P., Falcão, P.W., Pessoa, F.L.P., Cardozo-Filho, L., 2011. Vapor-liquid equilibrium of carbon dioxide + ethanol: experimental measurements with acoustic method and thermodynamic modeling. J. Thermodyn. 2011, 1–11. https://doi.org/10.1155/2011/251075.

Oliveira, C.S.D.D., Moreira, P., Resende, J., Cruz, M.T., Pereira, C.M.F.F., Silva, A.M.S.S., Santos, S.A.O.O., Silvestre, A.J.D.D., 2020. Characterization and cytotoxicity assessment of the lipophilic fractions of different morphological parts of *Acacia dealbata*. Int. J. Mol. Sci. 21, 1814. https://doi.org/10.3390/ijms21051814.

Pereira, R.G., Nakamura, R.N., Rodrigues, M.V.N., Osorio-Tobón, J.F., Garcia, V.L., Martinez, J., 2017. Supercritical fluid extraction of phyllanthin and niranthin from Phyllanthus amarus Schum. & Thonn. J. Supercrit. Fluids 127, 23–32. https://doi.org/10.1016/j.supflu.2017.03.017.

Perrut, M., 2000. Supercritical fluid applications: industrial developments and economic issues. Ind. Eng. Chem. Res. 39, 4531–4535. https://doi.org/10.1021/IE000211C/ASSET/IMAGES/LARGE/IE000211CF00001.JPEG.

Poling, B.E., Prausnitz, J.M., O'Connell, J.P., 2001. The Properties of Gases and Liquids, 5th ed. McGraw-Hill, New York. https://doi.org/10.1036/0070116822.

Rodrigues, M.F.F., Sousa, I.M.O., Vardanega, R., Nogueira, G.C., Meireles, M.A.A., Foglio, M.A., Marchese, J.A., 2019. Techno-economic evaluation of artemisinin extraction from Artemisia annua L. using supercritical carbon dioxide. Ind. Crops Prod. 132, 336–343. https://doi.org/10.1016/J.INDCROP.2019.02.049.

Rodrigues, V.H., de Melo, M.M.R., Portugal, I., Silva, C.M., 2018. Supercritical fluid extraction of *Eucalyptus globulus* leaves. Experimental and modelling studies of the influence of operating conditions and biomass pretreatment upon yields and kinetics. Sep. Purif. Technol. 191, 173–181. https://doi.org/10.1016/j.seppur.2017.09.026.

Rodrigues, V.H., de Melo, M.M.R., Portugal, I., Silva, C.M., 2019. Simulation and techno-economic optimization of the supercritical CO_2 extraction of *Eucalyptus globulus* bark at industrial scale. J. Supercrit. Fluids 145, 169–180. https://doi.org/10.1016/j.supflu.2018.11.025.

Rodrigues, V.H., de Melo, M.M.R., Portugal, I., Silva, C.M., 2021a. Lupane-type triterpenoids from *Acacia dealbata* bark extracted by different methods. Ind. Crops Prod. 170, 113734 https://doi.org/10.1016/j.indcrop.2021.113734.

Rodrigues, V.H., de Melo, M.M.R., Portugal, I., Silva, C.M., 2021b. Extraction of added-value triterpenoids from *Acacia dealbata* leaves using supercritical fluid extraction. Processes 9, 1159. https://doi.org/10.3390/pr9071159.

Rodrigues, V.H., de Melo, M.M.R., Tenberg, V., Carreira, R., Portugal, I., Silva, C.M., 2021c. Similarity analysis of essential oils and oleoresins of *Eucalyptus globulus* leaves produced by distinct methods, solvents and operating conditions. Ind. Crops Prod. 164, 113339 https://doi.org/10.1016/j.indcrop.2021.113339.

Saleem, M., 2009. Lupeol, a novel anti-inflammatory and anti-cancer dietary triterpene. Cancer Lett. 285, 109–115. https://doi.org/10.1016/j.canlet.2009.04.033.

Santos, S.A.O.O., Villaverde, J.J., Silva, C.M., Neto, C.P., Silvestre, A.J.D.D., 2012. Supercritical fluid extraction of phenolic compounds from *Eucalyptus globulus* Labill bark. J. Supercrit. Fluids 71, 71–79. https://doi.org/10.1016/j.supflu.2012.07.004.

Sarkar, T., Tiwari, S., Rawat, K., Solanki, P.R., Bohidar, H.B., 2017. Hydrophilic, fluorescent and superparamagnetic iron oxide-carbon composite nanoparticles. Colloids Surf. A Physicochem. Eng. Asp. 514, 218–225. https://doi.org/10.1016/j.colsurfa.2016.11.061.

Takishima, S., Saiki, K., Arai, K., Saito, S., 1986. Phase equilibria for CO_2-C_2H_5OH-H_2O system. J. Chem. Eng. Jpn. 19, 48–56. https://doi.org/10.1252/jcej.19.48.

The Navigator Company, 2021. Relatório & Contas 2020.

Turton, R., Bailie, R.C., Whiting, W.B., Shaeiwitz, J.A., Bhattacharyya, D., 2012. Analysis, Synthesis, and Design of Chemical Processes, 4th ed. Prentice Hall.

Wagner, Z., Pavlíček, J., 1994. Vapour-liquid equilibrium in the carbon dioxide—ethyl acetate system at high pressure. Fluid Phase Equilib. 97, 119–126. https://doi.org/10.1016/0378-3812(94)85010-0.

Xu, F., Huang, X., Wu, H., Wang, X., 2018. Beneficial health effects of lupenone triterpene: a review. Biomed. Pharmacother. 103, 198–203. https://doi.org/10.1016/j.biopha.2018.04.019.

Yeo, S.-D., Park, S.-J., Kim, J.-W., Kim, J.-C., 2000. Critical properties of carbon dioxide + methanol, + ethanol, + 1-propanol, and + 1-butanol. J. Chem. Eng. Data 45, 932–935. https://doi.org/10.1021/je000104p.

Zabot, G.L., Moraes, M.N., Meireles, M.A.A., 2018. Process integration for producing tocotrienols-rich oil and bixin-rich extract from annatto seeds: a techno-economic approach. Food Bioprod. Process. 109, 122–138. https://doi.org/10.1016/j.fbp.2018.03.007.

Zaird, B., 2022. GitHub - zmeri/PC-SAFT: Functions implementing the PC-SAFT equation of state, including association, electrolyte and dipole terms [WWW Document]. URL ⟨https://github.com/zmeri/PC-SAFT?fbclid=IwAR1alen3FFv-SllsAuqkmZ6IEpVfaSzBFu-FU0dDaW0b3oJ-rKGCC3nIWVE⟩ (Accessed 19 October 2021).